

RESEARCH

Open Access



# Two waves of evolution in the rodent pregnancy-specific glycoprotein (*Psg*) gene family lead to structurally diverse PSGs

Robert Kammerer<sup>1\*</sup> and Wolfgang Zimmermann<sup>2,3</sup>

## Abstract

**Background** The evolution of pregnancy-specific glycoprotein (PSG) genes within the CEA gene family of primates correlates with the evolution of hemochorial placentation about 45 Myr ago. Thus, we hypothesized that hemochorial placentation with intimate contact between fetal cells and maternal immune cells favors the evolution and expansion of PSGs. With only a few exceptions, all rodents have hemochorial placentas thus the question arises whether *Psgs* evolved in all rodent genera.

**Results** In the analysis of 94 rodent species from 4 suborders, we identified *Psg* genes only in the suborder Myomorpha in three families (characteristic species in brackets), namely Muridae (mouse), Cricetidae (hamster) and Nesomyidae (giant pouched rat). All *Psgs* are located, as previously described for mouse and rat, in a region of the genome separated from the *Cea* gene family locus by several megabases, further referred to as the rodent *Psg* locus. In the suborders Castorimorpha (beaver), Hystricognatha (guinea pig) and Sciuromorpha (squirrel), neither *Psg* genes nor so called CEA-related cell adhesion molecule (*Ceacam*) genes were found in the *Psg* locus. There was even no evidence for the existence of *Psgs* in any other genomic region. In contrast to the *Psg*-harboring rodent species, which do not have activating CEACAMs, we were able to identify *Ceacam* genes encoding activating CEACAMs in all other rodents studied. In the *Psg* locus, there are genes encoding three structurally distinct CEACAM/PSGs: (i) CEACAMs composed of one N- and one A2-type domain (CEACAM9, CEACAM15), (ii) composed of two N domains (CEACAM11-CEACAM14) and (iii) composed of three to eight N domains and one A2 domain (PSGs). All of them were found to be secreted glycoproteins preferentially expressed by trophoblast cells, thus they should be considered as PSGs.

**Conclusion** In rodents *Psg* genes evolved only recently in the suborder Myomorpha shortly upon their most recent common ancestor (MRCA) has coopted the retroviral genes syncytin-A and syncytin-B which enabled the evolution of the three-layered trophoblast. The expansion of *Psgs* is limited to the *Psg* locus most likely after a translocation of a CEA-related gene – possibly encoding an ITAM harboring CEACAM. According to the expression pattern two waves of gene amplification occurred, coding for structurally different PSGs.

**Keywords** Pregnancy-specific glycoprotein (PSG), carcinoembryonic antigen (CEA), Carcinoembryonic antigen-related cell–cell adhesion molecule (CEACAM), Immunoglobulin superfamily, Rodents, Trophoblast, Hemochorial placenta

\*Correspondence:  
Robert Kammerer  
Robert.Kammerer@fli.de  
Full list of author information is available at the end of the article



## Background

Pregnancy-specific glycoproteins (PSGs) were first described in humans as proteins in the serum of pregnant women [1]. Subsequently, the genes which encode human PSGs were identified and found to be members of the carcinoembryonic antigen (*CEA*) gene family which by itself is a member of the immunoglobulin gene superfamily [2, 3]. Once the *CEA* gene families were investigated in mice and rats a subgroup of the gene products was identified as secreted glycoproteins that were predominantly expressed by trophoblast cells and were named as PSGs in rodents [4–6]. Surprisingly, the structure of rodent PSGs differs significantly from that of human PSGs [6]. While human PSGs are composed of one N terminal immunoglobulin variable (IgV)-like domain (also called, N domain) and two to three immunoglobulin constant (IgC)-like domains (two A and one B domains) murine PSGs contain three to eight N domains followed by a single IgC domain of the A2-type found among others in CEACAM1 [7]. This led to the assumption that primate and rodent PSGs evolved independently in both orders. More recently, we found that in some microbat species, putative PSGs exist, composed of a single N domain followed by a single A domain [8]. Furthermore, in horses PSGs consisting of a single N domain were identified [9]. Despite the vast structural differences, common functions were described for PSGs of different species such as inhibition of platelet aggregation, activation of latent TGF $\beta$  and other immunomodulating functions [9–13] suggesting that PSGs developed independently in different mammalian lineages by convergent evolution [14]. This raises the question about the driving force of PSG evolution within the *CEA* gene family. Based on the fact that humans, mice, and rats as well as the above-indicated bat species have a hemochorial placenta, where fetal trophoblast cells have direct contact with maternal immune cells we and others hypothesized that PSGs evolved to regulate maternal immunity against fetal antigens [15, 16]. Indeed, it was found that equine PSGs were expressed by highly invasive trophoblast cells the so-called girdle cells which later form endometrial cups, a unique structure in equine placenta [9]. It is well documented that these cells are recognized by the maternal immune system which is also expected for trophoblast cells in mammals with hemochorial placentation [17]. Furthermore, in primates PSGs were found only in species with hemochorial placentas but not in primates that have an epitheliochorial placenta further pointing to an association of PSG evolution and intimate interaction of fetal trophoblast cells and the maternal immune cells [16]. Rodents, with only very few exceptions, have a hemochorial placenta, so we wondered when the PSGs evolved in rodents [18].

Rodents first appear in the fossil record at the end of the Paleocene and earliest Eocene, about 54 million years ago (mya) [19]. Nowadays, the order Rodentia comprises about 40% of all mammalian species [20] and is divided into five suborders, the Anomaluromorpha (e.g. springhares), Castorimorpha (e.g. beavers and kangaroo rats), Myomorpha (e.g. mice and hamsters), Hystricomorpha (e.g. guinea pigs and chinchillas) and the Sciuromorpha (e.g. squirrels and mountain beavers) [21]. Mice and rats belong to the Myomorpha suborder which appeared ~26 mya. The *Mus-Rattus* split is estimated to have occurred 8.8 to 10.3 mya ago [22]. Since PSGs in mice and rats are thought to have a common ancestor this indicates that PSGs in rodents evolved at least about 10 mya ago. But what happened during the remaining 40 million years of rodent existence? To answer this question, we investigated the *CEA* gene families in 94 rodent species containing members of the rodent suborders Myomorpha, Hystricomorpha, Sciuromorpha, and Castorimorpha. We found only supporting evidence for the evolution of PSGs in Muroidea, a subgroup of the Myomorpha, but not in other rodents. The key event for the amplification of PSGs was most likely the translocation of *CEA* gene family member(s) or parts of them from the *CEA* gene family locus into the *Npas1/Pglyrp1* locus. In this locus three, structurally different members of the *CEA* gene family could be found which all encode secreted glycoproteins. PSGs consists of multiple N domains and a single A domain, CEACAM11–14 consists of two N domains, and CEACAM9 and CEACAM15 are composed of one N domain and one A domain. According to their expression pattern in mice, all of them have to be considered to be functional PSGs. Thus, domain arrangements of PSGs do not only differ fundamentally between species but also within a single species.

## Results

### Recent evolution of pregnancy-specific glycoproteins in rodents

*Psgs* are well described for mice and rats but so far not for other rodents. In mice and rats, *Psgs* are located in the genome locus flanked by marker genes *Npas1* and *Pglyrp1* [23]. This locus will be further referred to as the “rodent *Psg* locus” in this publication. In contrast, no *CEA* gene family members are present in this region in primate genomes [16]. In mice, in addition to the 17 *Psgs* (*Psg16*–*Psg32*) *Ceacam9* and *Ceacam11–15* are located at this locus [7, 24]. To get first insights into the evolution of *Psgs* in rodents, other than mice and rats, we used the sequences of the above-mentioned mouse genes to identify *Psgs* in the genome of 94 rodent species using the Basic Local Alignment Search Tool (BLAST) and the NCBI and Ensemble databases (Fig. 1, Supplementary

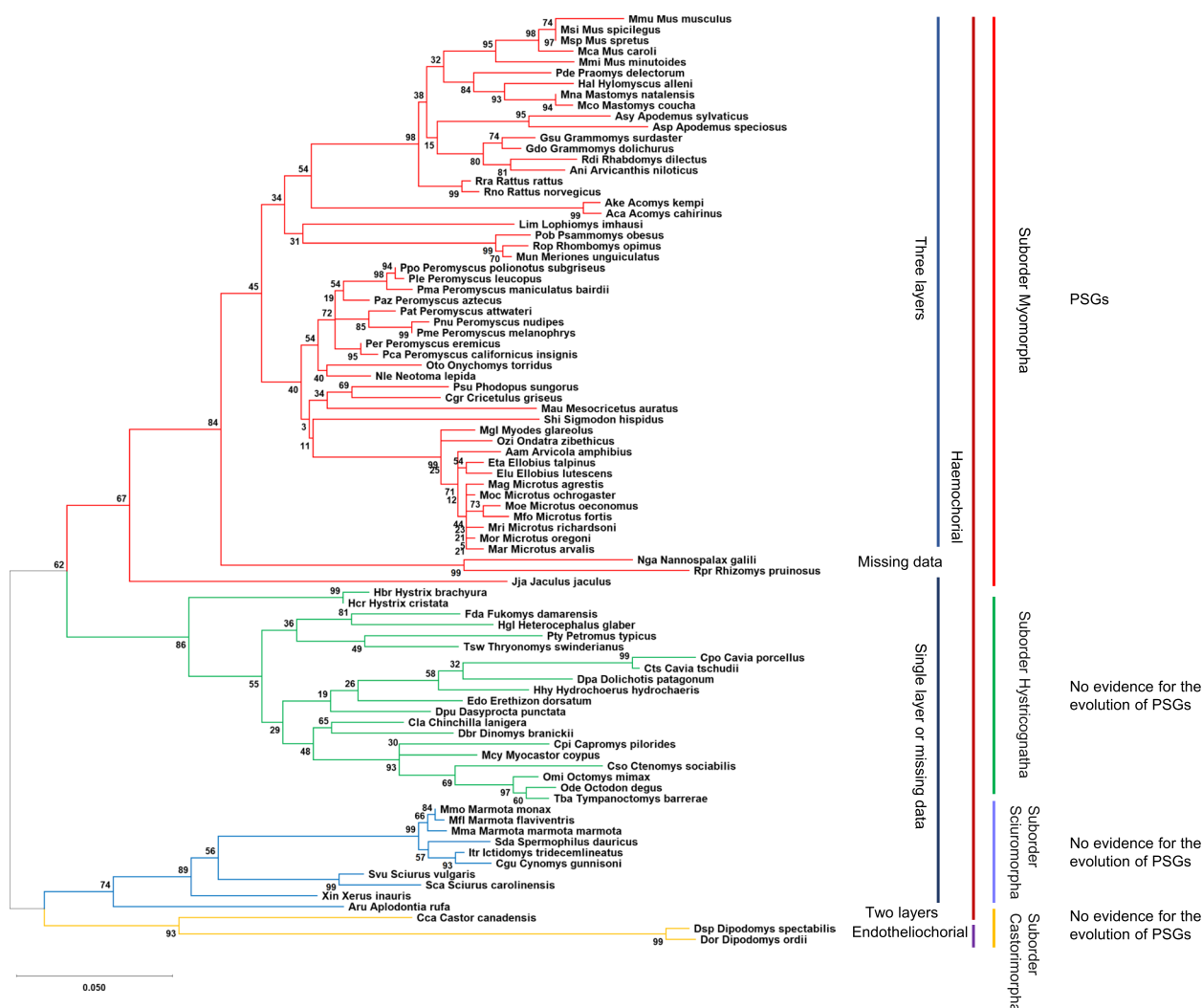


**Fig. 1** Phylogeny of the analyzed rodent species. To depict the phylogeny of the analysed rodent species we generated the gene tree using the nucleotide sequence of the conserved *Ceacam19* gene, since the gene trees of *Ceacam19* were previously found to resemble closely the species trees in various mammalian orders [7, 16, 23]. The phylogenetic tree was constructed using the N domain exon nucleotide sequences of *Ceacam19* genes. The color of the branches indicates the suborder to which the species belong (further indicated on the right side by vertical lines). The number of placental layers and the type of placenta are indicated on the right. The presence of *Psg* genes is indicated

Table 1). *Psgs* as described for mice and rats, as well as homologs to *Ceacam9*, 11–15 were identified only in the suborder Myomorpha but not in the suborders Castorimorpha, Hystricomorpha and Scuriomorpha (Fig. 1).

*Psgs* were found in all analyzed species of the suborder Myomorpha except in the genome of the lesser Egyptian jerboa (*Jaculus jaculus*; Dipoditae) and the two members of the Spalacidae family the Upper Galilee mountains blind mole rat (*Nannospalax galili*) and the hoary bamboo rat (*Rhizomys pruinosus*) (Fig. 2). Thus, the presence of *Psgs* is limited to three rodent families (Cricetidae, Muridae and Nesomyidae) of the Muroidea clade. Interestingly, the number of *Psgs* varied widely from three

genes in the genome of the African giant pouch rat (*Cricetomys gambianus*) a member of the Nesomyidae family and of the Mongolian gerbil (*Meriones unguiculatus*), the great gerbil (*Rhombomys opimus*) and the fat sand rat (*Psammomys obesus*) all three are members of the Gerbillinae subfamily, to 25 genes (including 2 pseudogenes) in the North American deer mouse (*Peromyscus maniculatus*; Neotominae subfamily) (Fig. 2). Interestingly, in all rodent species where we identified *Psgs* we also identified *Ceacam9* orthologs, although in the three Gerbillinae species (*Meriones unguiculatus*, *Rhombomys opimus*, *Psammomys obesus*) *Ceacam9* seem to be a pseudogene due to a common two nucleotide deletion in the N

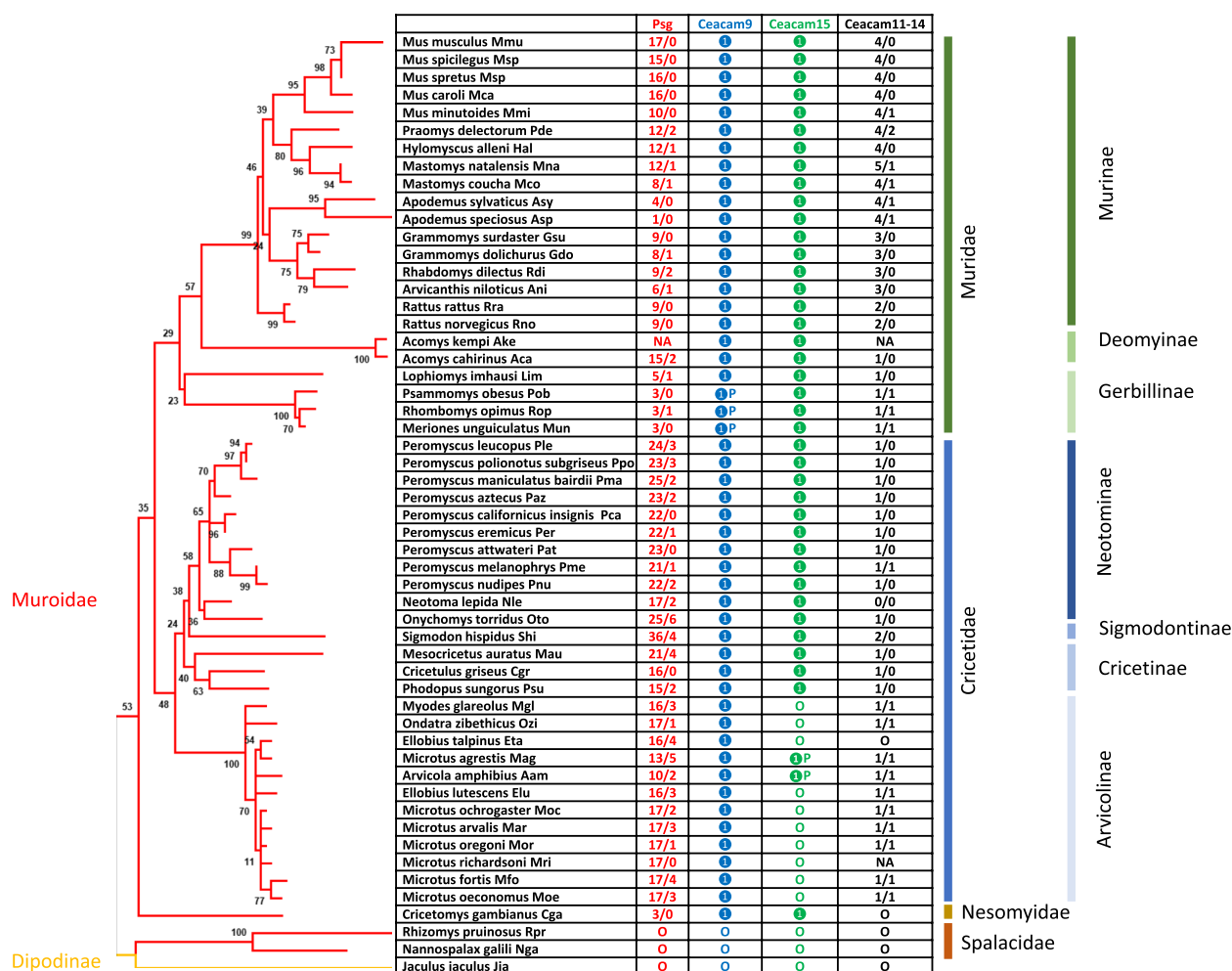


**Fig. 2** Psgs evolved in the clade Muroidea. The phylogenetic relationship of the analysed species is indicated by the gene tree constructed with the nucleotide sequences of the *Ceacam19* N domain exons. The presence of genes found in the genome locus flanked by marker genes *Npas1* and *Pglyrp1* in mice were analysed in 54 species of the suborder Myomorpha. Open circles indicate that the gene was not found in the genome; filled circles specify that the gene was identified in the genome as a single copy; P next to the filled circle indicates that the gene is a pseudogene according to our definition (Material and Methods). NA = not analysed; The numbers indicate the total number of genes identified/ the number of genes expected to represent pseudogenes

domain exon (Fig. 2). *Ceacam15* orthologs were found in all species which have *Psgs* and *Ceacam9* except in species of the Arvicolinae subfamily (Figs. 1 and 2). However, a possible remnant of *Ceacam15* was found in the two *Ellobius* species as well as in the genome of *M. glareolus* and *O. zibethicus*, indicating that *Ceacam15* was lost in the Arvicolinae subfamily. In species that do not have *Psg* genes, neither *Ceacam9* orthologs nor *Ceacam15* orthologs were found (Fig. 2). Genes related to murine *Ceacam11-14* are found in a subgroup of the species with *Psgs* and are described in more detail below.

**Coincidence of *Psg* appearance at the “rodent *Psg* locus” and loss of ITAM-encoding *Ceacams* in rodent *CEA* gene families**

In order to get further information about the possible origin of *Ceacam*-related genes at the rodent *Psg* locus we analysed the chromosomal arrangement of *Ceacam*-related genes. Selected species for which available scaffolds were long enough to cover the entire *Ceacam/Psg* locus are depicted in Fig. 3. Remarkably, species which lack *Psgs* do also not harbor any other members of the *Cea* gene family in the “rodent *Psg* locus” (Fig. 3). This was verified for species belonging to the Suborders Hystricomorpha (*n*=6), Sciuromorpha (*n*=5), Castriomorpha (*n*=2) as well as to the members of the

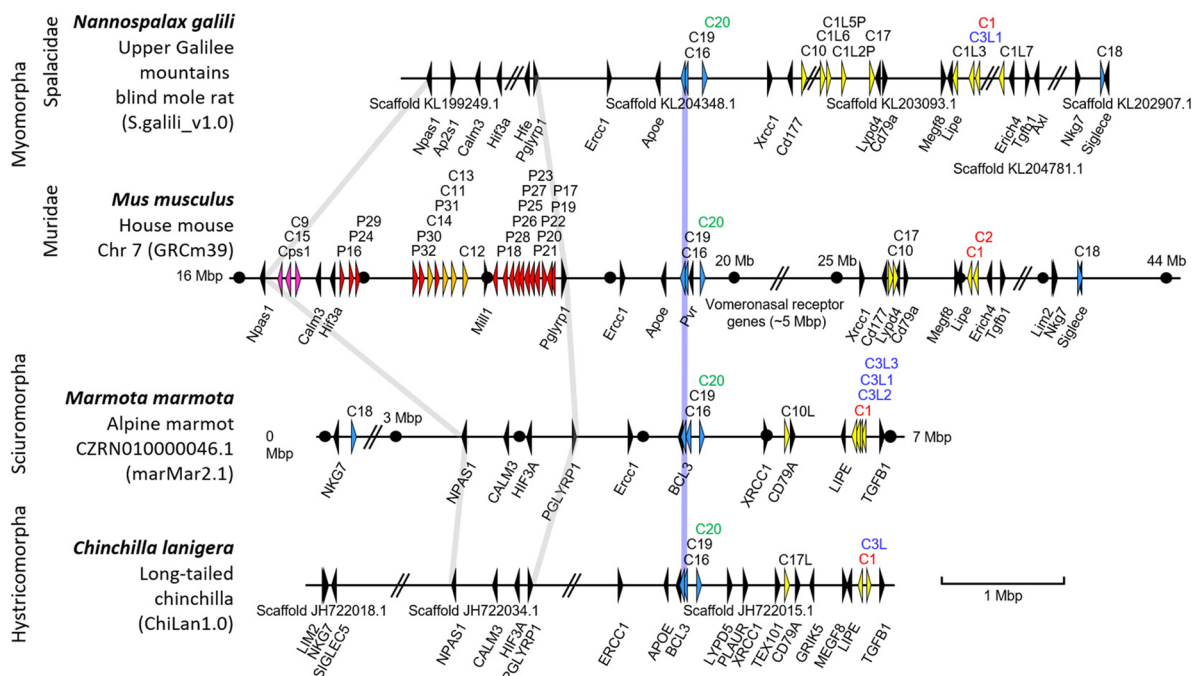


**Fig. 3** Evolution of *Psgs* in rodents is restricted to the *Npas1/Pglyrp1* locus. The chromosomal arrangements of *Ceacam*-related genes of selected species of the Myomorpha (*Nannospalax galili*, *Mus musculus*), Sciuromorpha (*Marmota marmota*), and Hystricomorpha (*Chinchilla lanigera*) suborders are shown. Arrowheads indicate genes with their transcriptional orientation. The *Psg*-related genes are shown in red (*Psg*), purple (*Ceacam9*, *Ceacam15*, and *Ceacam* pseudogene 1, *Cps1*) or orange (*Ceacam11-14*), *Ceacam1*-related *Ceacam* genes in yellow, conserved *Ceacam* genes in blue and selected flanking genes in black. The *Ceacam* gene loci were aligned along the position of *Ceacam16* (blue line). Gray lines were used to delineate the *Npas1/Pglyrp1* loci. Abbreviated names of *Ceacam1*-like genes with ITIM/ITSM-encoding exons are shown in red and with ITAM and ITAM-like motif-encoding exons in green and blue, respectively. Nucleotide numbering of the chromosomes starts at the telomere. Selected positions 1 Mbp apart are indicated by dots. Databases and their versions used are listed below the species name. The borders of scaffolds are indicated by double slashes, their names below the chromosome. The exact distances between the scaffolds still have to be determined by complete whole genome sequencing. Of note: The rodent genomes (except the murine genome) are not completely sequenced yet. Therefore, not all *Ceacam* genes identified in whole genome shotgun (WGS) databases have been found in the published assembled genomes. C, *Ceacam*; Cps, *Ceacam* pseudogene; C1L(P), *Ceacam1*-like (pseudo)gene, the same abbreviation schema applies to similar abbreviations; Mbp, million base pairs; P, pregnancy-specific glycoprotein (*Psg*) genes

Spalacidae family ( $n=2$ ) (Fig. 3, data not shown). This may indicate that a single translocation of one or more *Cea* gene family members gave rise to the evolution of all *Cea* gene family members in the “rodent *Psg* locus”. However, in the *Ceacam* locus diverse differences and copy number variations could be observed. Interestingly, we observed that rodent species which do not have *Cea* gene family members in the “rodent *Psg* locus” have *Cea* gene family members encoding CEACAMs which have activating signaling motifs in the cytoplasmic tails (Fig. 3, Supplementary file 1, data not shown). Of note such *Ceacams* were not found in rodent species in which *Psgs* evolved including mice and rats. In some species e.g. the alpine marmot (*Marmota marmota*) and the woodchuck (*M. monax*) such genes even have been multiplied (Fig. 3, Supplementary file 1). This may tempt to speculate that an activating *Ceacam* was destroyed and subsequently lost due to the translocation of a *Ceacam* gene to form

the “rodent *Psg* locus” in the MRCA of *Psg* harboring rodents.

### A second wave of gene amplification led to the generation of murine *Ceacam11-14* genes

To further delineate the evolution of the *Ceacam*-related genes at the “rodent *Psg* locus” we performed phylogenetic analyses of N domain exons of members of different muroid families i.e. house mouse and Chinese hamster, using their nucleotide sequences. An orthologous relationship was found for *Ceacam9*, *Ceacam15*, *Ceacam16*, *Ceacam17* and *Ceacam19* (Fig. 4). Furthermore, mouse *Ceacam1*, *Ceacam2* and *Ceacam10N1* are closely related with *Ceacam1* and *Ceacam2* in the Chinese hamster (*Cricetulus griseus*) but did not exhibit pairwise orthology. For *Psgs* the N1 domain exon sequences build a cluster but no orthologous relationship between individual *Psgs* of the two species could be identified. The N2 and N3-6 N domains did not segregate completely into

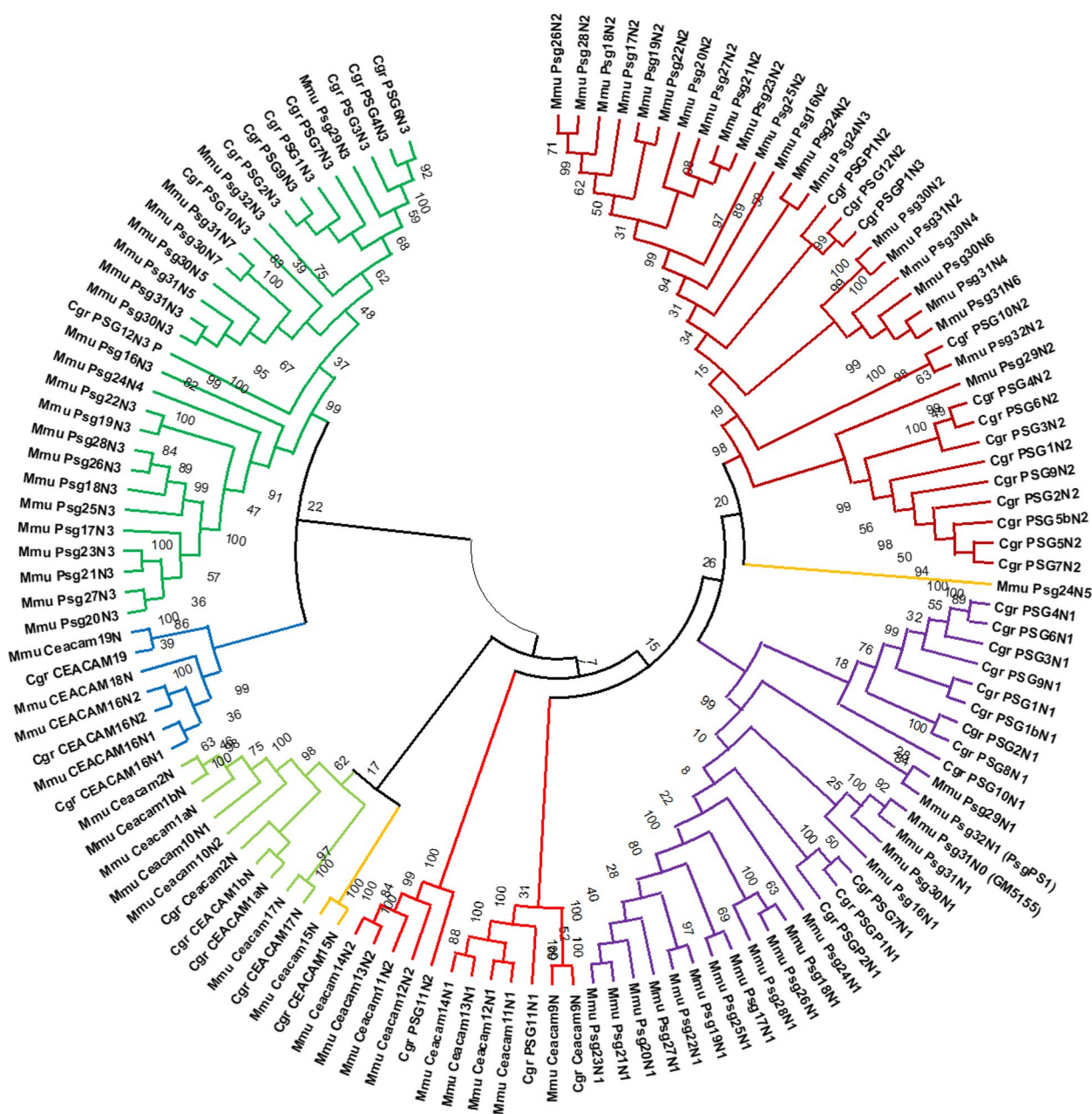


**Fig. 4** Phylogenetic tree of *Ceacam*/*Psg*-related N domain exon nucleotide sequences of *Mus musculus* (house mouse) and *Cricetus griseus* (Chinese hamster). The phylogenetic tree was constructed using the maximum likelihood (ML) method and Hasegawa-Kishino-Yano model [25] with bootstrap testing (500 replicates). The bootstrap consensus tree inferred from 500 replicates is taken to represent the evolutionary history of the exons analyzed. The percentage of replicate trees in which the associated exons clustered together in the bootstrap test is shown next to the branches. Initial tree(s) for the heuristic search were obtained automatically by applying Neighbor-Joining and BioNJ algorithms to a matrix of pairwise distances estimated using the Maximum Composite Likelihood (MCL) approach, and then selecting the topology with superior log likelihood value. Multi-alignment of N domain exon sequences was performed using Muscle implemented in MEGAX. For murine *Psg31* and *Psg32* the name which is currently annotated in the NCBI and Ensemble databases are indicated in brackets. Three letter code abbreviation for species: Mmu, *Mus musculus*; Cgr, *Cricetus griseus*

individual clusters indicating that recent exon duplication and shuffling has taken place during expansion of *Psgs*. Remarkably, in the consensus tree the *Ceacam9* N

domain exon is closely related to the N1 domain exons of *Ceacam11-14* in mice and to a *Ceacam11*-like gene in the hamster. In addition, the N2 sequence of murine

*Ceacam11-14* cluster together with the N2 domain of the *Ceacam11*-like gene in the hamster. However, hamster C11-like exons N1 and N2 do not exhibit clear orthology to any of the *Ceacam11-14* genes. Together, this indicates that murine *Ceacam11-14* genes and the hamster *Ceacam11*-like gene have a common ancestor (Fig. 4).

Therefore, we used the nucleotide sequences of the *Ceacam11*-like gene in the hamster to search for closely related N domain exons in other rodent species. With a few exceptions, we identified one to four *Ceacam11*-like genes (composed of two N domain exons) in all species that also have *Psg* and *Ceacam9* genes. A single *Ceacam11*-like gene was found in species of the Cricetidae, Neotominae, and Deomyinae rodent subfamilies. In Murinae an amplification of the *Ceacam11*-like gene had occurred, leading to two genes in rats, three genes in *Grammomys*, *Arvicanthis*, and *Mastomys*, and four genes in the *Mus* genus (Figs. 2 and 5). In Arvicolinae, only *Ceacam11*-like gene remnants (N2 exons) could be identified. This indicates that this gene was lost in Arvicolinae. Like in the *Psg* genes, orthologous relationship can only be observed in closely related rodent species.

#### Structure of rodent CEACAM11-14

*Ceacam11-14* genes are in general composed of four exons which encode the leader sequence, the N1 domain, the N2 domain and a 3' exon harboring the stop codon. Murine *Ceacam14* has a mutation in the splice donor site of exon 3 leading to the usage of a stop codon immediately after the splice donor site. Interestingly, we could not identify exon 4 from rodents with only 1 *Ceacam11*-like gene, however, the splice donor site of exon 3 is intact. Structurally, *Ceacam12* is the most remarkable since the domain encoded by exon 4 is predicted to be part of the ligand binding face of domain N2 which is formed by one of the two  $\beta$ -sheets present in IgV-like domains. This structure is well conserved between different species, indicating that there may exist a common ligand for CEACAM12 (Fig. 6).

#### *Ceacam11-14* genes are preferentially expressed in trophoblast cells

PSGs are defined as CEACAM1-related CEACAMs that are secreted and preferentially expressed in trophoblast cells [26]. Previously, we found that murine *Ceacam11-14* are expressed in placental tissues in the mouse [7]. Here we substantiated these findings by additional analyses of publicly available data sets as described in “Material and Methods”. Genes of the *Cea* gene family that were preferentially expressed in the placenta include *Ceacam9*, *Ceacam11-14*, and the *Psg* genes as determined by bulk mRNAseq data (Fig. 7A). scRNAseq data revealed that each of these genes is preferentially but not exclusively

expressed by trophoblast cells in mice (Fig. 7B). In particular, *Ceacam14*, *Psg21*, *Psg23*, *Psg27*, and *Psg30* are expressed by additional tissue compartments in the placenta (Fig. 7B).

We further analyzed the expression of murine *Psgs* and *Psg-like Ceacams* by different trophoblast cell types at day 9.5, 10.5, 12.5 and 14.5 of pregnancy at single cell resolution. Overall murine *Psgs* and *Psg-like Ceacam* genes have a diverse expression pattern, although most genes were preferentially expressed by spongiotrophoblast cells and their precursors. However, in particular *Ceacam9* and *Psg29* were also expressed by glycogen cells. In addition, a significant expression of most *Psgs* and *Psg-like Ceacams* in syncytiotrophoblast cells and their precursors was noticed. *Psg23* showed the broadest expression pattern being expressed in different trophoblast cell types. *Ceacam15*, *Psg20*, *Psg22* and *Psg26* showed only a weak expression in placental cells at the investigated developmental stages. The expression of the majority of *Psgs* increased during pregnancy. In contrast, *Ceacam9* and *Psg29* showed the highest expression on day 9.5 followed by a decrease of expression. *Psg24* reached a peak of expression on day 10.5 (Fig. 8). *Ceacam11-14* showed a very similar expression pattern although with significant differences of expression intensities at the mRNA level (Fig. 8). Together this expression analyses strongly indicate that all *Ceacam/Psg* genes at the “rodent *Psg* locus” have to be considered as functional *Psgs*.

#### The evolution of *Psgs* in Muroidea is highly dynamic

Variation of *Psg* copy numbers within Muroidea indicates a highly dynamic evolution of *Psg* genes in the *Psg* gene locus. However, there are significant differences between groups of *Psg/Psg-like Ceacam* genes. *Ceacam9* and *Ceacam15* are well-conserved single-copy genes. *Ceacam9* is found in all *Psg*-containing species. In some closely related Muroidea species (*M. unguulates*, *P. obesus*, *R. opimus*) *Ceacam9* appears to be a pseudogene due to a common 2 bp deletion in the N exons (Fig. 2; data not shown). In contrast, *Ceacam15* has been lost in the entire Arvicolinae subfamily (only *Ceacam15* gene remnants can be found in some Arvicolinae species: *Elu*, *Eta*, *Mgl*, *Ozi*). *Ceacam11* has been conserved for a certain time during which no amplification occurred. Only recently this gene has been amplified in Murinae. The *bona fide* *Psg* genes have been subject to multiple rounds of gene duplications and exon shuffling. Interestingly, gene expansion (possibly followed by gene loss in some groups of species) happened differentially at different subregions of the *Psg* locus of Muroidea species. While the number of *Psg*-like genes varies little in the *Psg* subregion flanked by the marker genes *Hif3a* and *Mill1* (9–12 *Psg* and *Ceacam11-14* genes), there is a large variation in

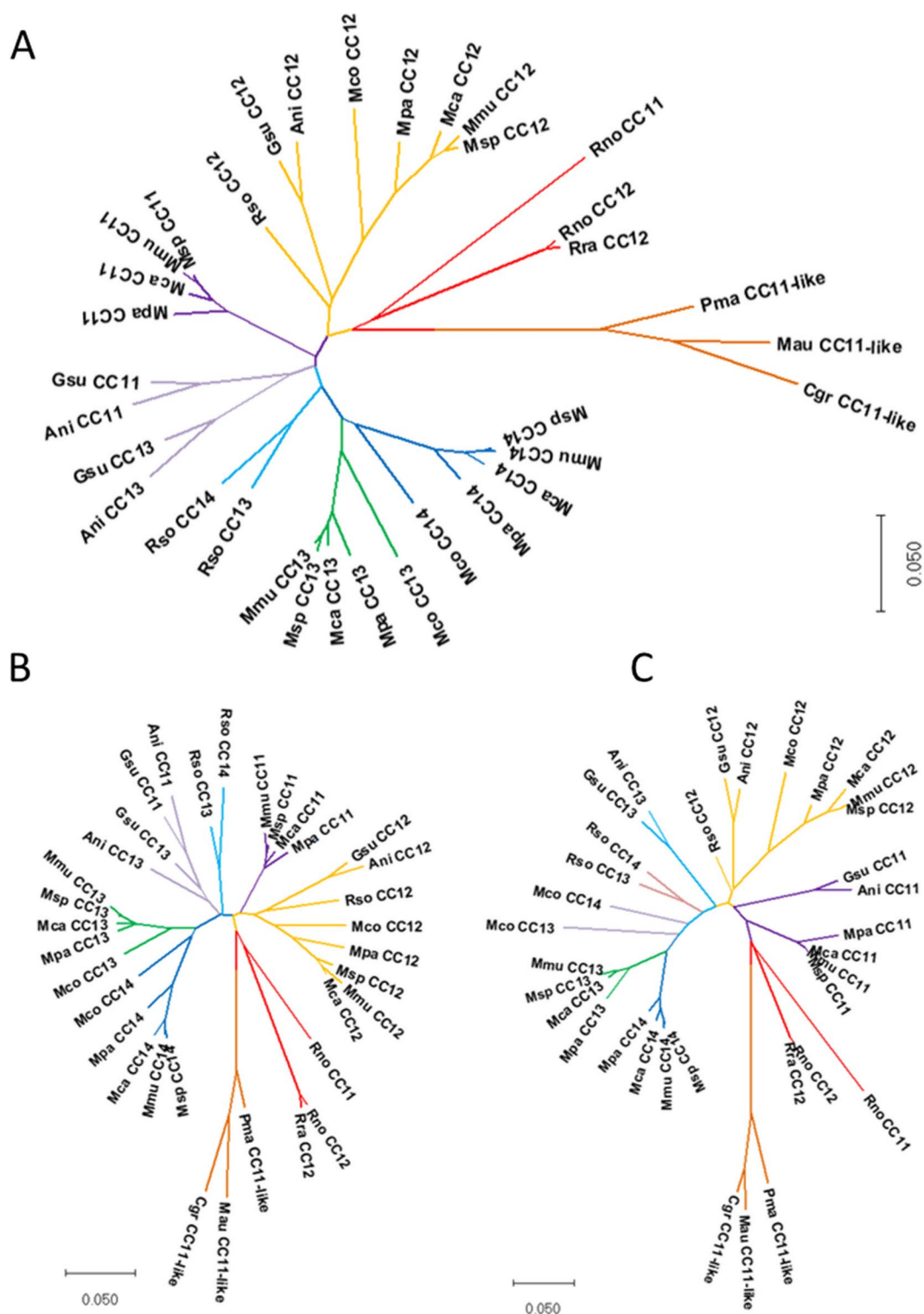


**Fig. 5** Phylogeny of the *Ceacam11-14* genes in rodents. Nucleotide sequences of the complete coding sequence (A) the N1 exon (B) and the N2 exon (C) of the *Ceacam11-14* genes were used for phylogenetic analysis. The evolutionary history was inferred by using the Maximum Likelihood method and the Tamura 3-parameter model. The species abbreviations are explained in Fig. 1 and Supplementary Table 1. CC, Ceacam



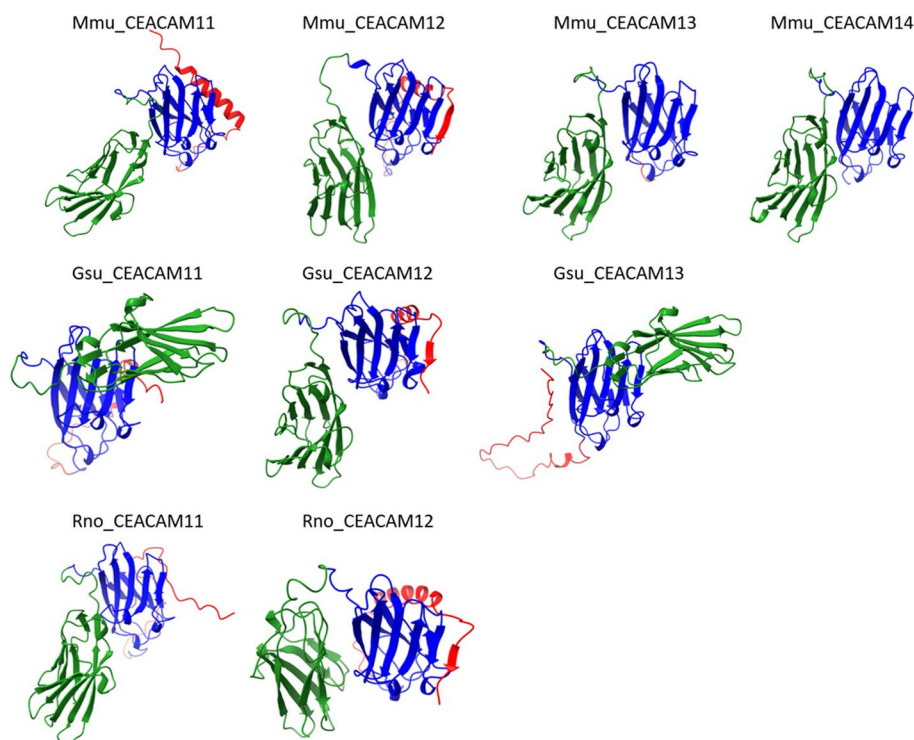


**Fig. 6** Structure of the expanded CEACAM11-related CEACAMs. The structure of the CEACAM11-related CEACAMs from mouse (Mmu), African thick rat (Gsu) and rat (Rno) was predicted using ColabFold. The N1 domains are shown in green the N2 domains in blue and the exon 4-encoded domain in red. The arrows represent  $\beta$ -strands

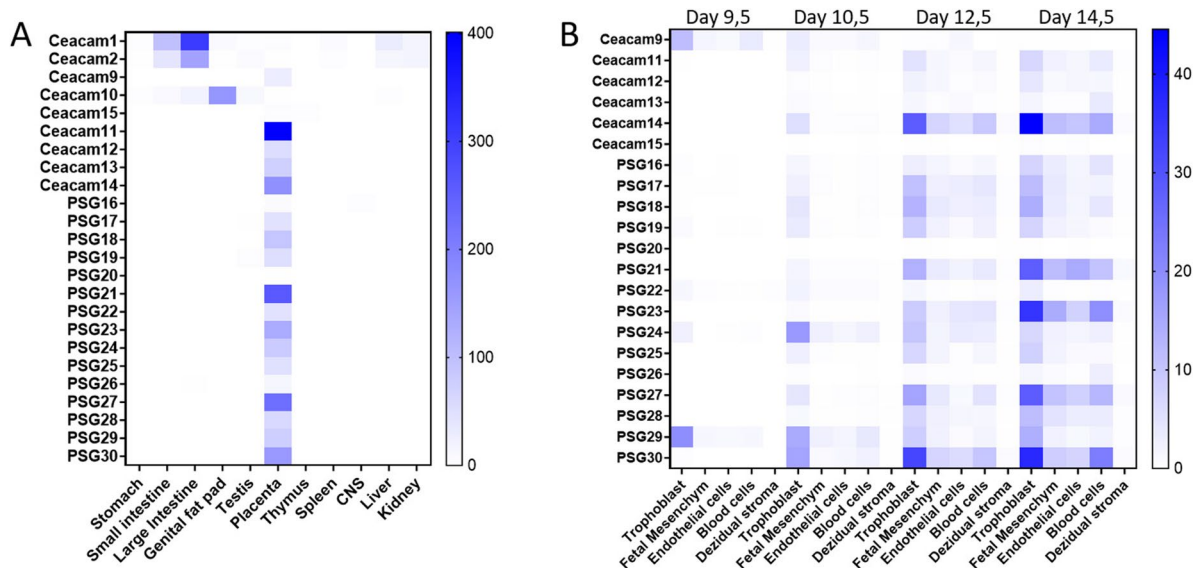


**Fig. 7** Expression of murine *Cea* gene family members. **A** Expression of murine *Cea* gene family members in different tissues as extracted from the Mouse ENCODE project (NCBI Geo BioProject: PRJNA66167). The relative expression is based on bulk mRNAseq and indicated by the color code as depicted on the right. **B** Expression of placenta-specific *Cea* gene family members by different placental cell types as determined by scRNAseq [27]. The relative expression is indicated by the color code as depicted on the right

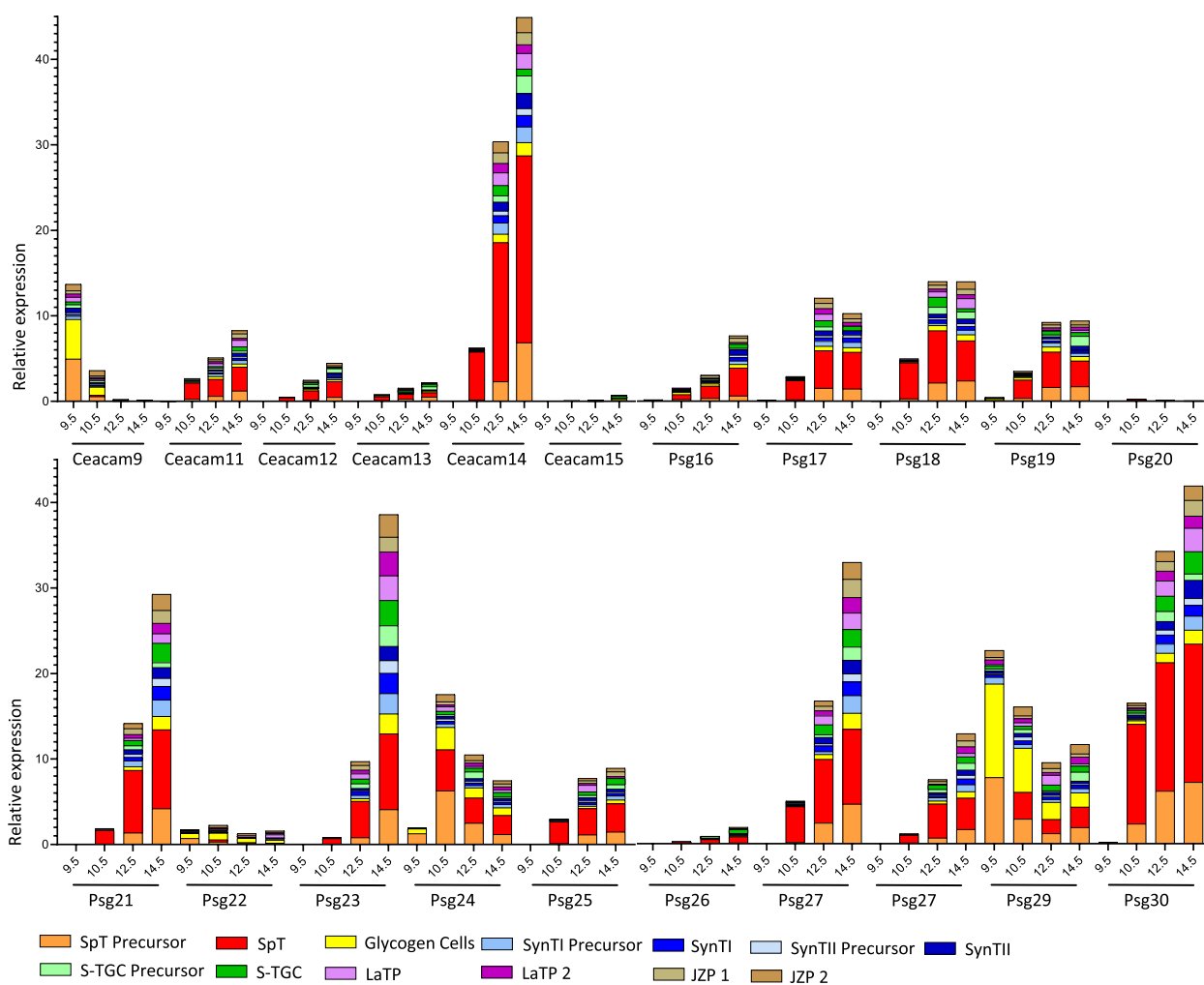


**Fig. 8** Relative expression of *Cea* gene family members in trophoblast subpopulations. The color code that identifies the different cell populations is shown below the graph. SpT, Spongiotrophoblast; SynTI1, outermost syncytiotrophoblast layer, SynTI2, syncytiotrophoblast layer between SynTI1 and the fetal endothelium; S-TGC, sinusoidal trophoblast giant cells; LaTP, labyrinth trophoblast progenitor; JZP, Junctional zone precursor [27]

*Psg* gene numbers in the *Psg* subregion flanked by *Mill1* and *Pglyrp1*, where between 1 (*M. coucha*) and 11 *Psgs* (*M. musculus*) are found (Fig. 9). In contrast, most of *Psg* gene size expansion by exon duplications occurred at the *Hif3a/Mill1* subregion (Fig. 9). Taken together, this complex evolutionary history makes the assignment of orthologous genes almost impossible between different families of Muroidea.

**The structure of PSG/PSG-like CEACAMs in rodents**

Two principle domain compositions of PSGs/PSG-like CEACAMs were found in rodents, one group consist of two N domains and the other is built by one A domain and a variable number of N domains. Intact PSG-like CEACAMs built of two N domains are absent in various groups of rodents, including Nesomyidae, Avricolinae, and Gerbillinae (Fig. 10). The dominant domain

composition of rodent PSGs is three N domains combined with one A domain (some 85%), followed by PSGs comprising five N domains and one A domain (Fig. 10). Nevertheless, in each species analyzed at least one member is composed of one N domain and one A domain (Fig. 10).

**Variable evolutionary selection on individual genes and rodent populations**

Previously we found that *PSGs* in bats after amplification are under selection for diversification. In primates, we observed a largely variable selection pattern depending on the species and domain examined. Here, we selected closely related groups of rodents where an orthologous relationship between genes could be identified and performed dN/dS analyses. Three rodent subfamilies could be analyzed Murinae, Neotominae, and Arvicolinae

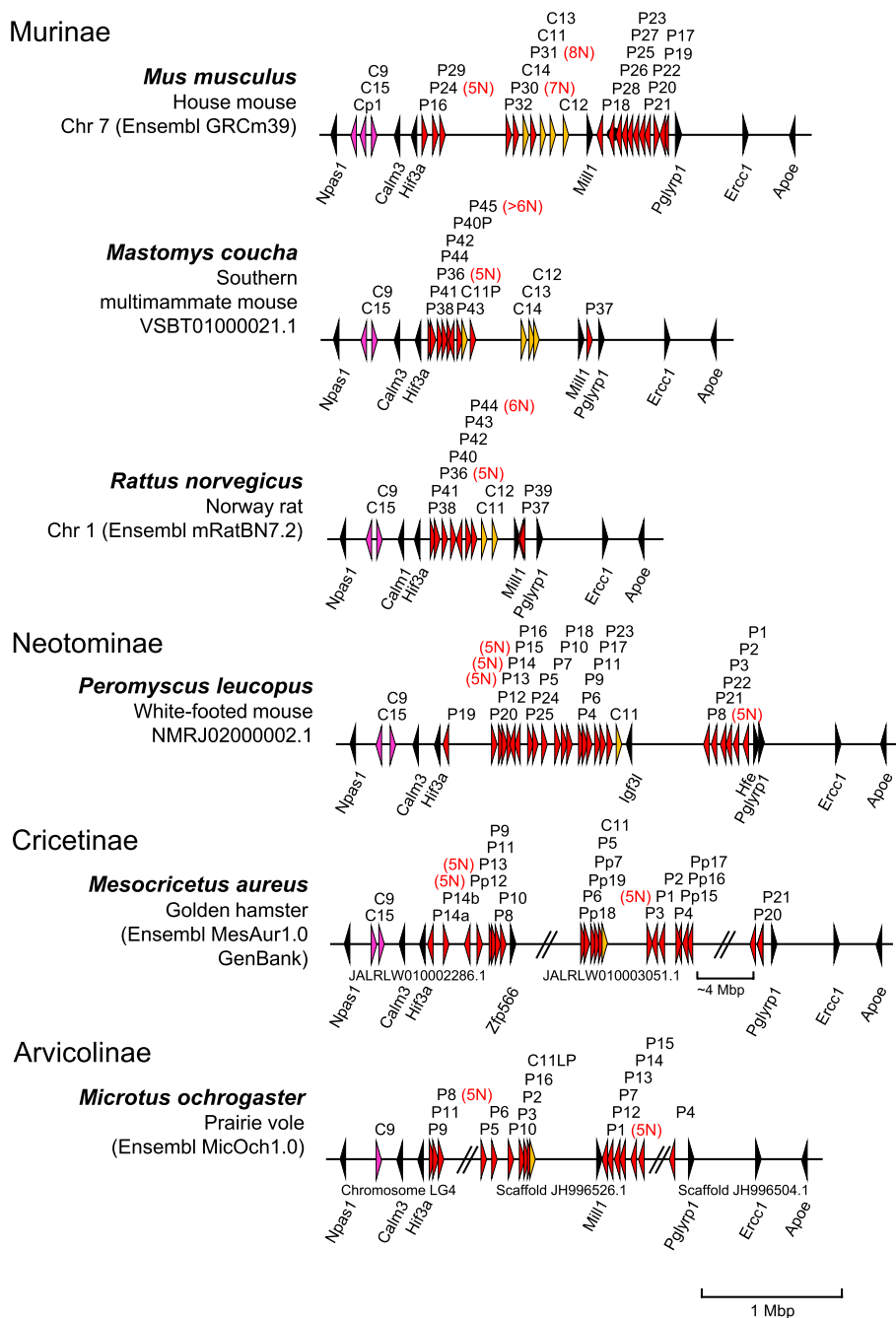


**Fig. 9** Divergent evolution of the *Psg* locus in Muroidea. The chromosomal arrangements of *Psg* genes at the *Npas1*/*Pglyrp1* locus of selected species of the Muroidea clade are shown. Subfamily and species names are shown at the left side. Arrowheads indicate genes with their transcriptional orientation. The *Psg*-related genes are shown in red (*Psg*), purple (*Ceacam9*, *Ceacam15* and *Ceacam pseudogene 1*, *Cp1*) or orange (*Ceacam11-14*), and selected flanking genes in black. The number of IgV domain-encoding N exons exceeding the standard number 3 is indicated in brackets next to the gene names in red. IgV variant order as found in *Mmu\_Psg24* and *Asp\_Psg31* are shown in red and blue color, respectively. The *Psg* gene loci were aligned along the position of the *Npas1* gene. Chromosomal location (where available), databases and their versions used are listed below the species name. The borders of scaffolds are indicated by double slashes, their names below the chromosome. Of note: ortholog assignment of *Ceacam11-14* genes between species is not possible due to lack of unequivocal synteny and sequence relationship. Therefore, same gene names do not imply an orthologous relationship. *Asp*, *Apodemus speciosus*; *C*, *Ceacam*; *Cps*, *Ceacam pseudogene*; *Mbp*, million base pairs; *Mmu*, *Mus musculus*; *P*, pregnancy-specific glycoprotein (*Psg*) genes; *Pp*, *Psg* pseudogene

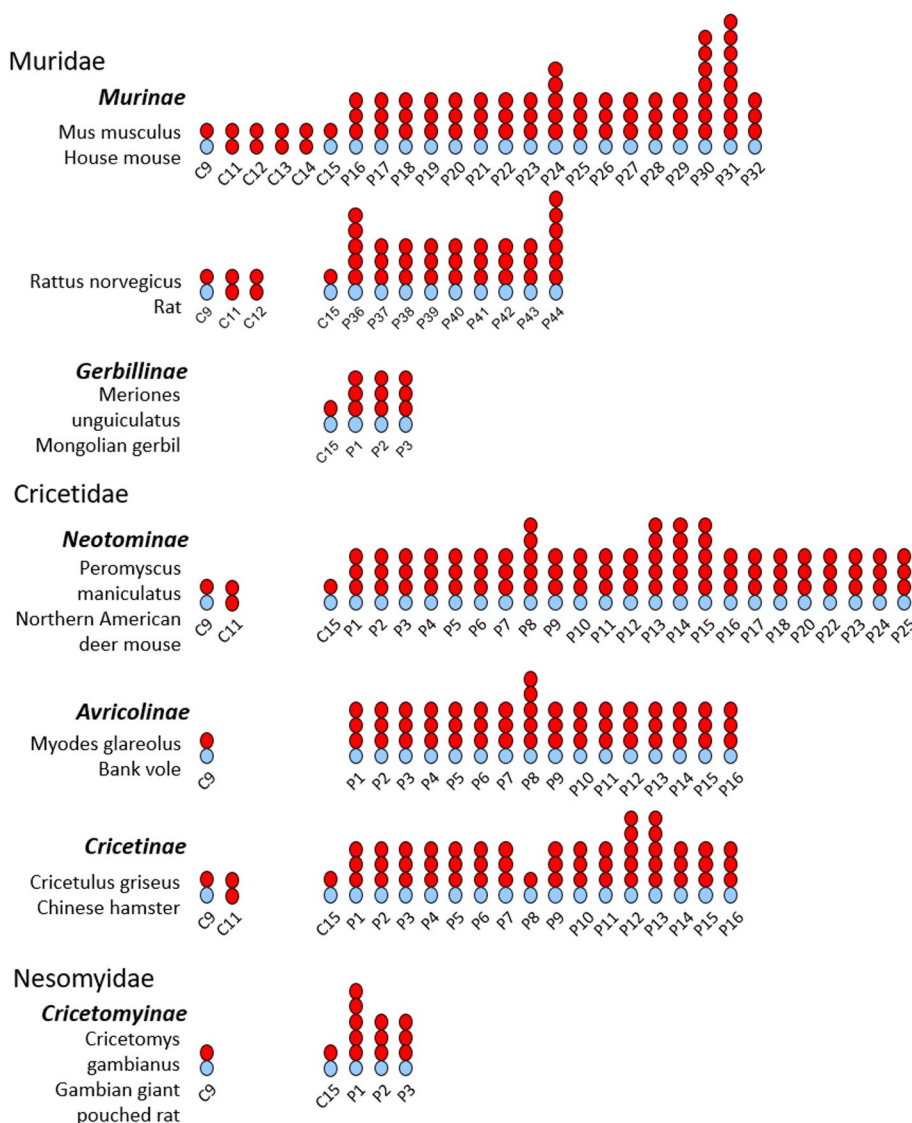


**Fig. 10** Domain structure of rodent PSGs/PSG-like CEACAMs. The domain organization of PSG/PSG-like CEACAMs from selected rodent species from the Muridae, Cricetidae, and Nesomyidae families was predicted by gene analysis. Family, subfamily and species names are indicated at the left side. Mouse and rat PSG domain organizations were confirmed by EST sequences when available. IgV-like domains are shown as red, and IgC-like domains as blue ovals. Note the highly variable number of PSG in the different rodent species (between 3 and 23). Identical PSG numbering does not imply an orthologous relationship. C, CEACAM; P, PSG

(See figure on next page.)

**Fig. 11** Differential selection for diversification in Ig domain exons of trophoblast-specific *Ceacam*/*Psg* genes. Nucleotide sequences of N and A domain exons of *Psg* orthologs from rodent species **A-C**: Murinae (Ani, Asy, Gsu, Hal, Mca, Mco, Mmi, Mmu, Mmu\_cas, Mmu\_mus, Mna, Mpa, Msi, Msp, Pde, Rdi, Rno, Rra), **D**: Neotominae (Nle, Oto, Pat, Paz, Pca, Per, Ple, Pma, Pme, Pnu, Ppo) and **G**: Avricolinae subfamilies (Elu, Eta, Mag, Mar, Mfo, Mgl, Moc, Moe, Mor, Ozi) were compared pair-wise in all combinations after manual removal of gaps and the ratio of the rate of nonsynonymous (dN) and synonymous mutations (dS) was calculated for whole N and A domain exons and the mean ratios were plotted. The whiskers represent standard errors of the mean (SEM). Only genes were included for which an orthologous relationship could be demonstrated by phylogenetic analyses using CLUSTALW. The dN/dS values of three to five *Psg* genes for each exon type and subfamily were averaged and plotted (**B, E, H**). In addition, the dN/dS ratios for the N domain exons of trophoblast-specific *Ceacam* genes and, for comparison, for *Ceacam1* and *Ceacam19* orthologs of the same rodent species were calculated (**C, F, I**). These two genes are known to represent genes under diversifying (dN/dS > 1) and purifying selection (dN/dS < 1), respectively, in other mammalian species [23]. Of note: In Neotominae species, for the single gene related to the *Ceacam11-14* genes in Murinae no ortholog could be clearly identified. A, IgC-like domain exon; N, N domain exon; *Ceacam11*, CEACAM11-like. For the three letter species name abbreviations please refer to Supplementary Table 1

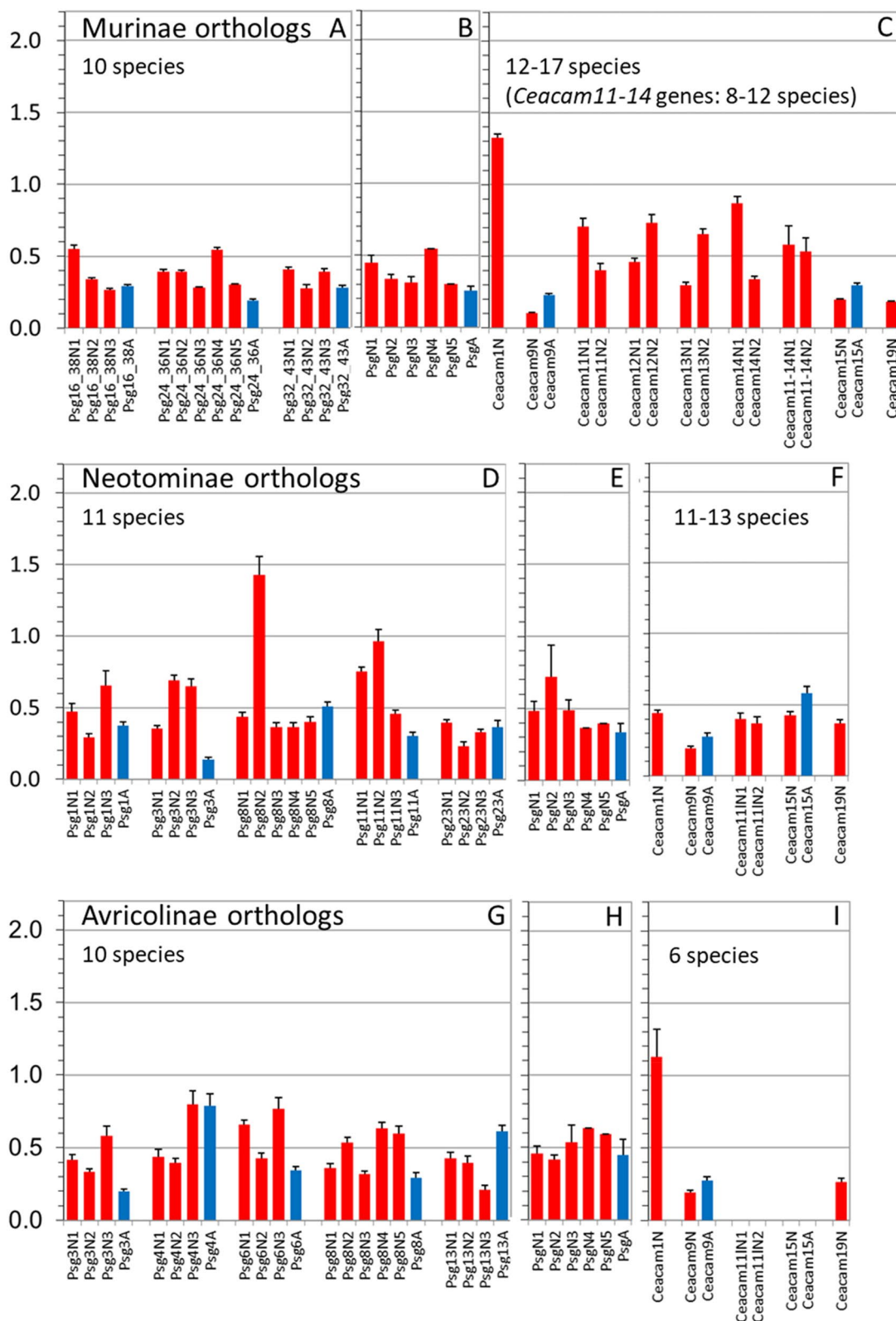


**Fig. 11** (See legend on previous page.)

(Fig. 11). In all groups we found that *Ceacam9* is highly conserved i.e., under purifying selection ( $dN/dS < 1$ ) mostly even more than the conserved *Ceacam19* gene (Fig. 11C, F, I). In contrast, the N domain of *Ceacam1* is under selection for diversification (positive selection) in Murinae and Arvicolinae while it is under purifying selection (negative selection) in Neotominae (Fig. 11C, F, I) indicated by  $dN/dS$  values  $> 1$  and  $< 1$ , respectively. Remarkably, the positive selection of the *Ceacam1* N domain exon in Murinae as in other species (e.g. humans) is thought to be the result of pathogen usage of CEACAM1 as an entry receptor. In general, PSGs in rodents are under negative selection (Fig. 11A, B, D, E, G, H). In Neotominae and Arvicolinae individual N domains and A domains show a relaxation of negative selection. In particular, the N2 domains of PSG8 and PSG11 in Neotominae exhibit or are close to positive selection, respectively. In Arvicolinae several N and A domain exons show a relaxed negative selection ( $0.5 < dN/dS < 1.0$ ) (Fig. 11G, H). The single *CEACAM11-14* gene in Neotominae is under negative selection ( $dN/dS = \sim 0.4$ ), in contrast in Murinae the *Ceacam11-14* genes show some relaxation of purifying selection, indicating that upon amplification the newly generated genes underwent some adaptation to their new functions (Fig. 11C).

#### Independent evolution of *Psgs* in rodents without a “rodent *Psg* locus”?

Since structurally different *Psgs* evolved in Muroidea it is worth speculating that in other rodents *Psgs* evolved at a different locus in the genome as found for Muroidea. Indeed, we found some amplification of *Ceacams* at the *Ceacam* locus flanked by the marker genes *Cd79a* and *Xrcc1* (Fig. 3, data not shown). However, there is no evidence that these genes represent *bona fide* genes that encode secreted proteins or are expressed in a trophoblast-specific manner. In contrast, in species where we further analyzed the expanded *Ceacams* we found also an expansion of transmembrane domain coding exons, suggesting that these encode membrane-bound CEACAMs.

#### Discussion

PSGs were so far described in primates, mice and rats, microbats, and the horse [9, 14, 16]. With the exception of the horse, these species have a hemochorial placenta. Thus, we have previously speculated that the intimate contact of trophoblast cells with maternal immune cells drives the evolution of PSGs [11, 16, 23]. Indeed, in primates, the emergence of PSGs correlates with the appearance of hemochorial placentation [16]. The only primates so far identified that have a hemochorial placenta but no PSGs are the tarsiers [16] indicating that in primates PSGs evolve almost in parallel to a hemochorial type of

placentation. However, while the amplification of PSG genes in New World monkeys remained limited (1–7 PSG genes) a massive amplification occurred in Old World monkeys resulting in more than 20 gene copies in some species [16]. These differences may be due to unknown restrictions of successful gene duplication at the PSG locus in New World monkeys or by a relaxed selection pressure for PSG gene amplification. In order to get further insights into the evolution of PSG genes we analyzed the evolution of *Psgs* in rodents. Since all rodents, with very few exceptions, have a hemochorial placenta we expected that in most if not all rodents *Psgs* are present, although they have been only described in mice and rats so far. It has been suggested that the common ancestor of rodents had a hemochorial placentation with an interhemal barrier that had a single layer of syncytial trophoblast cells [18]. This anatomical feature was retained in the clade comprising Hystricomorpha (guinea pigs and others) and Sciuromorpha (squirrels) [18]. In contrast, in Myomorpha (mice and others) several placental transformations occurred [18], most remarkably within the Muridae family, which has a special three-layered trophoblast [28, 29]. The three-layered trophoblast containing a layer of cytotrophoblast and two layers of syncytiotrophoblast cells appeared together with the capture of the *syncytin-A* and *syncytin-B* genes in the most recent common ancestor (MRCA) of Muroidea including Muridae, Cricetidae, and Spalacidae family species [30]. Of them, the Spalacidae is the only family in which *Psgs* did not evolve indicating that shortly after the invention of the three-layered trophoblast *Psgs* evolved. This may refine our picture of the forces driving PSG development. It may be that alterations of the fetomaternal interface create opportunities to optimize the molecular fetomaternal crosstalk. Members of the CEA family may be predisposed to fulfill this task once they are secreted by fetal trophoblast cells. Such a “beneficial” PSG gene may then be fixed in the genome and eventually amplified. Because the fetomaternal interface evolves extraordinarily fast such changes may frequently occur thus explaining why PSGs can evolve independently multiple times in different mammalian lineages. Since *Ceacam9*, *Ceacam15*, and *Ceacam11-like* genes or at least remnants of the latter are present in the genome of *Psg*-harboring rodents it is not possible to decide which ancestor of these genes is the primordial gene of rodent *Psgs*. However, a combination of *Ceacam9* or *Ceacam15* with *Ceacam11-14* would provide all building blocks (three N domain exons and one A domain exon) to create typical rodent *Psgs*. The strong correlation between the existence of *Psgs* and the presence of *Ceacam9* may indicate that *Ceacam9* plays a pivotal role in the evolution of *Psg* genes. If *Ceacam9* is the founder of *Psgs*, *Ceacam15* may be an early duplicate

of *Ceacam9* which gained a new function but was not further amplified. The high conservation of *Ceacam15* argues for such a speculation. On the other hand, *Ceacam15* and the ancestor of *Ceacam11-14* were lost in Arvicolinae indicating that in the MRCA of this group, both genes lost their function and therefore were subsequently deleted from the genome. Rodent PSGs are in general composed of three (more rarely of five, six, seven or eight) IgV-like domains and one A domain of the A2 type. Since the vast majority of rodent *Psgs* are composed of the typical exon arrangement with 3 exons coding for IgV-like domains and one IgC-like domain we conclude that once a *Psg* gene had evolved the duplication of whole *Psg* genes was the major mechanism of *Psg* gene amplification in rodents. The expansion of PSGs is still ongoing as indicated by the different number of *Psg* genes and their independent expansion e.g. in mice and rats. In addition, as previously shown for mouse *Psgs*, *Psgs* of other Muroidea evolve extremely fast therefore orthologs can only be assigned between very closely related species (Fig. 4) [24]. The fast evolution limits the possibility to analyze the nature of selection on rodent *Psgs* (Fig. 11). Nevertheless, our results indicate that some *Psgs* in some species are under positive selection, but the majority are under purifying selection. These results suggest that most rodent PSGs have adapted to a certain function while only some, possibly newly duplicated, PSGs are free to acquire novel functions or ligands. More recently, a second wave of gene amplification took place. The ancestor of *Ceacam11-14* is under purifying selection in all species that have only one gene. In Murinae the purifying selection seems to be relaxed, enabling some flexibility for functional optimization (Fig. 11). Remarkably, CEACAM11-14 are structurally different from the bona fide PSGs in rodents composed of two N domains. However, the very similar expression pattern of *Ceacam11-14* and *Psgs* in placental cells (Figs. 7 and 8; [31]) suggest that both encode functional “PSGs”. We have previously reported that PSGs are structurally different in different species, due to an independent evolution. This is now the first report showing that PSGs did evolve twice in one mammalian group, leading to structurally distinct PSGs. This indicates that the birth of PSGs is a frequent event explaining the independent evolution in various mammalian lineages.

Since the translocation of a *Ceacam* gene family member or parts of it seem to be a hallmark of the evolution of *Psgs* in rodents the question arises what kind of *Ceacam* gene was translocated to form the original *Psg* locus? One possibility can be envisaged that part of an ITAM-containing *Ceacam* gene was translocated with concomitant destruction/loss of the ITAM motif-encoding region of the gene. Such a scenario would explain the strong

correlation between the absence of ITAM-containing CEACAMs and the presence of PSGs (Fig. 3). In rodents without PSGs, ITAM-containing CEACAMs exist, as in most other mammalian species (Fig. 3) [23]. Thus, this report shows for the first time that most rodents have ITAM-harboring CEACAMs and that the loss of ITAM-containing CEACAMs happened only recently affecting the species of the Muridae family. A summary of the possible evolution of *Psgs* in rodents is depicted in Fig. 12.

Although we did not find any evidence for the presence of PSG in other rodents we cannot exclude that they may exist in some species due to their structural variability and missing expression data of most species analyzed in this report. In addition, we are aware that the simplified construction of rodent phylogeny used in this study by comparing the IgV-like (N) domain exons of *Ceacam19* did not completely mirror the previously published studies using more complex molecular data [21, 22, 33]. In contrast to these studies, we did not see a monophyletic clade comprising Hystricomorpha and Sciuromorpha. In addition, the Castorimorpha did not appear to be a sister group of the Myomorpha as previously shown. Nevertheless, the relationship between the Muridae and Dipodidae as well as the relationship within the Muridae family agrees with published data [21, 22, 33].

In summary, the expansion of the analysis of the *CEA* gene family to the entire rodent clade shed new light on the evolution of the *CEA* gene family of the most frequently used animal models for medical research, i.e. mice and rats. This study demonstrates that the loss of an ITAM-encoding *Ceacam* gene and the appearance of *Psg* genes is a rather recent event in rodents only affecting the Cricetidae, Muridae and Nesomyidae families.

## Methods

### Identification and nomenclature of genes

Nucleotide and amino acid sequence searches were performed using the NCBI BLASTBLAT tools (<http://www.ncbi.nlm.nih.gov/BLAST>) and the Ensembl database (<http://www.ensembl.org/Multi/Tools/Blast?db=core>) using default parameters. For the identification of rodent *Ceacam* exons, *Ceacam* and *Psg* exon and cDNA sequences from known mouse and rat *Ceacam/Psgs* were used to search various databases at NCBI and Ensembl including whole-genome shotgun contigs (wgs), and Transcriptome Shotgun Assembly (TSA). A comprehensive overview of the used genomic data sources for the analyzed rodent species is given in Supplementary Table 1. Hits were considered to be significant if the E-value was  $< e^{-10}$  and the query cover was  $> 50\%$ . Genes that contained stop codons within their N domain exons or lacked appropriate splice acceptor and donor sites in

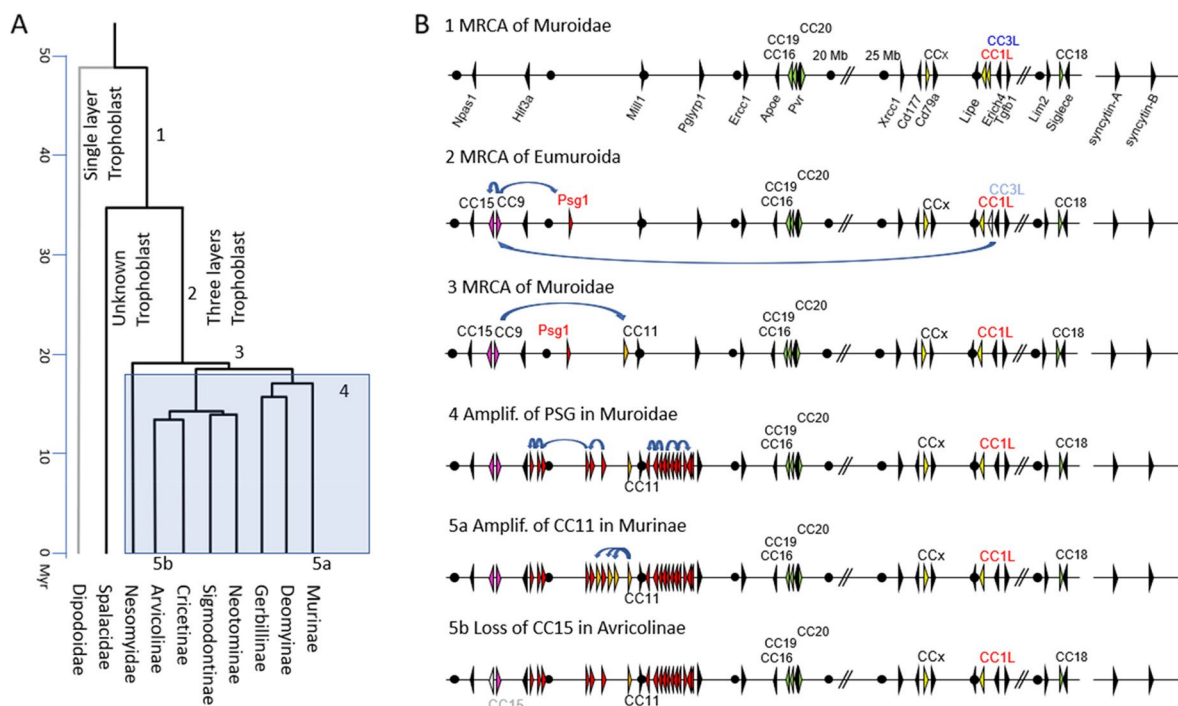


**Fig. 12** A proposed evolutionary path of rodent *PsGs*. The phylogenetic tree of the suborder Myomorpha is depicted in **A** (the gray shading indicates that in all lineages *PsGs* were amplified as shown in 4). The possible gene arrangement at the *Psg/Ceacam* locus of the MRCA as indicated with 1, 2, 3, 4, 5a and 5b is depicted in **B**. (1) The gene locus before *Ceacam* gene translocation. (2) The original gene locus upon *Ceacam* gene translocation (blue arrows). The arrowhead representing the CC3L gene is shown in pale color indicating that parts of it were translocated to the new „rodent *Psg* locus“. *Ceacam9* (CC9) is expected to be the original gene at the *Psg* locus followed by *Ceacam15* upon gene duplication and *Psg1* upon another gene duplication event and exon shuffling. (3) Creation of *Ceacam11* by gene duplication and exon shuffling. (4) Further expansion of the *Psg* genes by gene duplication of *Psg1* (first wave of *Psg* amplification). (5a) Amplification of *Ceacam11* in Murinae (second wave of *Psg* amplification). (5b) Loss of *Ceacam15* (shown in pale color) in Arvicolinae). The phylogenetic tree is drawn according to Steppan et al. [32]. CC, *Ceacam*; CC1L, *Ceacam1*-like; CCx, *Ceacam1*-related; Myr, million years; *Psg1*, pregnancy-specific glycoprotein gene 1

these exons were considered to represent pseudogenes. Nucleotide sequences from the N domain exons can be used as gene identifiers (Supplementary File 2). The same strategy was employed to identify other genes of the CEACAM families. *Ceacam* genes, the N exons of which exhibited >99% nucleotide sequence identity, were considered to represent alleles.

**Quantification of PSG expression**

For the quantification of murine PSG expression, we reanalyzed publicly available datasets, these include mRNA sequencing data sets generated by the Mouse ENCODE project available at NCBI Geo BioProject: PRJNA66167 as well as single cell mRNA sequencing data available at [https://figshare.com/projects/Single\\_nuclei\\_RNA-seq\\_of\\_mouse\\_placental\\_labyrinth\\_development/92354](https://figshare.com/projects/Single_nuclei_RNA-seq_of_mouse_placental_labyrinth_development/92354) [27, 34].

**Sequence motif identification and 3D modeling**

The presence of immunoreceptor tyrosine-based activation motifs (ITAM), ITAM-like, and immunoreceptor tyrosine-based inhibition motifs (ITIM) and immunoreceptor tyrosine-based switch motifs (ITSM) were confirmed using the amino acid sequence pattern search program ELM (<http://elm.eu.org/>). Transmembrane regions, and leader peptide sequences were identified using the TMHMM (<http://www.cbs.dtu.dk/services/TMHMM-2.0/>), the SignalP 4.1 programs (<http://www.cbs.dtu.dk/services/SignalP/>), respectively. The structure predictions of murine CEACAM11-14 and rat CEACAM11-12 were retrieved from the “Alpha-Fold Protein Structure Database”. The structure of CEACAM11-13 from African tree rat (*Grammomys surdaster*) was predicted using “ColabFold” [35].



## Phylogenetic analyses and determination of positive and purifying selection

Phylogenetic analyses based on nucleotide and amino acid sequences were conducted using MEGAX [36]. Sequence alignments were performed using Muscle [37] implemented in MEGAX. Phylogenetic trees were constructed using the maximum likelihood (ML) method with bootstrap testing (500 replicates). The best fit substitution model was selected within MEGAX. In order to determine the selective pressure on the maintenance of the nucleotide sequences, the number of nonsynonymous nucleotide substitution per nonsynonymous site (dN) and the number of synonymous substitutions per synonymous site (dS) were determined for *Psg* and *Ceacam* N domain and IgC-like exons. The dN/dS ratios between pairs of *Psg* orthologs and paralogs and orthologous *Ceacam* genes were calculated after manual editing of sequence gaps or insertions guided by the amino acid sequences using the SNAP program (Synonymous Nonsynonymous Analysis Program; <http://www.hiv.lanl.gov/content/sequence/SNAP/SNAP.html>) [38].

## Supplementary Information

The online version contains supplementary material available at <https://doi.org/10.1186/s12864-023-09560-6>.

**Additional file 1.**

**Additional file 2.**

**Additional file 3.**

## Acknowledgements

Not applicable

## Authors' contributions

R.K. conceived the study, carried out data analysis and drafted the manuscript. W.Z. performed most of the data mining and contributed equally to manuscript writing. Both authors read and approved the final manuscript.

## Funding

Open Access funding enabled and organized by Projekt DEAL. There was no specific funding source for this work.

## Availability of data and materials

The datasets analyzed during the current study are available in the NCBI and Ensembl repositories, <http://www.ncbi.nlm.nih.gov/> and <http://www.ensembl.org/index.html>. The accession numbers of the used genomic data of rodent species is described in "Supplementary Table 1". Nucleotide sequences from the N domains of newly described rodent genes, which can be used as gene identifiers for search in data bases are provided in "Supplementary File 2". Datasets supporting the conclusions of this article are included within this article and in additional files "Supplementary File 1" and Supplementary File 2". New sequencing data were not generated in this study.

## Declarations

### Ethics approval and consent to participate

Not applicable.

### Consent for publication

Not applicable.

## Competing interests

The authors declare no competing interests.

## Author details

<sup>1</sup>Institute of Immunology, Friedrich-Loeffler-Institute, Greifswald-Insel Riems, Greifswald, Germany. <sup>2</sup>Tumor Immunology Laboratory, LIFE Center, LMU Klinikum, University Munich, Munich, Germany. <sup>3</sup>Department of Urology, LMU Klinikum, University Munich, Munich, Germany.

Received: 29 March 2023 Accepted: 7 August 2023

Published online: 21 August 2023

## References

1. Bohn H. [Detection and characterization of pregnancy proteins in the human placenta and their quantitative immunochemical determination in sera from pregnant women]. *Arch Gynakol.* 1971;210(4):440–57.
2. Oikawa S, Inuzuka C, Kosaki G, Nakazato H. Exon-intron organization of a gene for pregnancy-specific beta 1-glycoprotein, a subfamily member of CEA family: implications for its characteristic repetitive domains and C-terminal sequences. *Biochem Biophys Res Commun.* 1988;156(1):68–77.
3. Streydio C, Lacka K, Swillens S, Vassart G. The human pregnancy-specific beta 1-glycoprotein (PS beta G) and the carcinoembryonic antigen (CEA)-related proteins are members of the same multigene family. *Biochem Biophys Res Commun.* 1988;154(1):130–7.
4. Chan WY, Tease LA, Bates JM Jr, Borjigin J, Shupert WL. Pregnancy-specific beta 1 glycoprotein in rat: tissue distribution of the mRNA and identification of testicular cDNA clones. *Hum Reprod.* 1988;3(5):687–92.
5. Ogilvie S, Shiverick KT, Larkin LH, Romrell LJ, Shupert WL, Chan WY. Pregnancy-specific beta 1-glycoprotein messenger ribonucleic acid and immunoreactive protein in the rat testis. *Endocrinology.* 1990;126(1):292–8.
6. Rudert F, Saunders AM, Rebstock S, Thompson JA, Zimmermann W. Characterization of murine carcinoembryonic antigen gene family members. *Mamm Genome.* 1992;3(5):262–73.
7. Zebhauser R, Kammerer R, Eisenried A, McLellan A, Moore T, Zimmermann W. Identification of a novel group of evolutionarily conserved members within the rapidly diverging murine cea family. *Genomics.* 2005;86(5):566–80. <https://doi.org/10.1016/j.ygeno.2005.07.008>.
8. Kammerer R, Mansfeld M, Hanske J, Missbach S, He X, Kollner B, Mouchantat S, Zimmermann W. Recent expansion and adaptive evolution of the carcinoembryonic antigen family in bats of the Yangochiroptera subgroup. *BMC Genomics.* 2017;18(1):717.
9. Aleksic D, Blaschke L, Missbach S, Hanske J, Weiss W, Handler J, Zimmermann W, Cabrera-Sharp V, Read JE, de Mestre AM, et al. Convergent evolution of pregnancy-specific glycoproteins in the human and horse. *Reproduction.* 2016;152(3):171–84.
10. Ballesteros A, Mentink-Kane MM, Warren J, Kaplan GG, Dveksler GS. Induction and activation of latent transforming growth factor-beta1 are carried out by two distinct domains of pregnancy-specific glycoprotein 1 (PSG1). *J Biol Chem.* 2015;290(7):4422–31.
11. Kammerer R, Ballesteros A, Bonsor D, Warren J, Williams JM, Moore T, Dveksler G. Equine pregnancy-specific glycoprotein CEACAM49 secreted by endometrial cup cells activates TGFβ. *Reproduction.* 2020;160(5):685–94. <https://doi.org/10.1530/REP-20-0277>.
12. Martinez FF, Cervi L, Knubel CP, Panzetta-Dutari GM, Motran CC. The role of pregnancy-specific glycoprotein 1a (PSG1a) in regulating the innate and adaptive immune response. *Am J Reprod Immunol.* 2013;69(4):383–94. <https://doi.org/10.1111/aji.12089>.
13. Warren J, Im M, Ballesteros A, Ha C, Moore T, Lambert F, Lucas S, Hinz B, Dveksler G. Activation of latent transforming growth factor-beta1, a conserved function for pregnancy-specific beta 1-glycoproteins. *Mol Hum Reprod.* 2018;24(12):602–12.
14. Moore T, Williams JM, Becerra-Rodriguez MA, Dunne M, Kammerer R, Dveksler G. Pregnancy-specific glycoproteins: evolution, expression, functions and disease associations. *Reproduction.* 2022;163(2):R11–23. <https://doi.org/10.1530/REP-21-0390>.

15. Moore T, Dveksler GS. Pregnancy-specific glycoproteins: complex gene families regulating maternal-fetal interactions. *Int J Dev Biol*. 2014;58(2–4):273–80.
16. Zimmermann W, Kammerer R. The immune-modulating pregnancy-specific glycoproteins evolve rapidly and their presence correlates with hemochorial placentation in primates. *BMC Genomics*. 2021;22(1):128. <https://doi.org/10.1186/s12864-021-07413-8>.
17. Lunn P, Vagnoni KE, Ginther OJ. The equine immune response to endometrial cups. *J Reprod Immunol*. 1997;34(3):203–16. [https://doi.org/10.1016/S0165-0378\(97\)00044-2](https://doi.org/10.1016/S0165-0378(97)00044-2).
18. Mess AM, Carter AM. Evolution of the interhaemal barrier in the placenta of rodents. *Placenta*. 2009;30(10):914–8. <https://doi.org/10.1016/j.placenta.2009.07.008>.
19. Meng J, Wyss AR, Dawson MR, Zhai R. Primitive fossil rodent from Inner Mongolia and its implications for mammalian phylogeny. *Nature*. 1994;370(6485):134–6. <https://doi.org/10.1038/370134a0>.
20. Connor J, Burgin JPC, Kahn PL, Upham NS. How many species of mammals are there? *J Mammal*. 2018;99(1):1–14.
21. Fabre PH, Hautier L, Dimitrov D, Douzery EJ. A glimpse on the pattern of rodent diversification: a phylogenetic approach. *BMC Evol Biol*. 2012;12:88.
22. Steppan S, Adkins R, Anderson J. Phylogeny and divergence-date estimates of rapid radiations in muroid rodents based on multiple nuclear genes. *Syst Biol*. 2004;53(4):533–53.
23. Kammerer R, Zimmermann W. Coevolution of activating and inhibitory receptors within mammalian carcinoembryonic antigen families. *BMC Biol*. 2010;8(1): 12. <https://doi.org/10.1186/1741-7007-8-12>.
24. McLellan AS, Fischer B, Dveksler G, Hori T, Wynne F, Ball M, Okumura K, Moore T, Zimmermann W. Structure and evolution of the mouse pregnancy-specific glycoprotein (psg) gene locus. *BMC Genomics*. 2005;6(1): 4. <https://doi.org/10.1186/1471-2164-6-4>.
25. Hasegawa M, Kishino H, Yano T. Dating of the human-ape splitting by a molecular clock of mitochondrial DNA. *J Mol Evol*. 1985;22(2):160–74.
26. Kammerer R, Herse F, Zimmermann W. Convergent evolution within CEA gene families in mammals: hints for species-specific selection pressures. Berlin: Springer; 2016.
27. Marsh B, Belloch R. Single nuclei RNA-seq of mouse placental labyrinth development. *Elife*. 2020;9:9. <https://doi.org/10.7554/eLife.60266>.
28. Enders AC. A comparative study of the fine structure of the trophoblast in several hemochorial placentas. *Am J Anat*. 1965;116(1):29–67. <https://doi.org/10.1002/aja.1001160103>.
29. King BF, Hastings RA 2. The comparative fine structure of the interhemal membrane of chorioallantoic placentas from six genera of myomorph rodents. *Am J Anat*. 1977;149(2):165–79. <https://doi.org/10.1002/aja.1001490204>.
30. Vernochet C, Redelsperger F, Harper F, Souquere S, Catzeflis F, Pierron G, Nevo E, Heidmann T, Dupressoir A. The captured retroviral envelope syncytin-A and syncytin-B genes are conserved in the Spalacidae together with hemotrichorial placentation. *Biol Reprod*. 2014;91(6):148.
31. Green MT, Martin RE, Kinkade JA, Schmidt RR, Bivens NJ, Tuteja G, Mao J, Rosenfeld CS. Maternal oxycodone treatment causes pathophysiological changes in the mouse placenta. *Placenta*. 2020;100:96–110. <https://doi.org/10.1016/j.placenta.2020.08.006>.
32. Steppan SJ, Schenk JJ. Muroid rodent phylogenetics: 900-species tree reveals increasing diversification rates. *PLoS ONE*. 2017;12(8):e0183070. <https://doi.org/10.1371/journal.pone.0183070>.
33. Swanson MT, Oliveros CH, Esselstyn JA. A phylogenomic rodent tree reveals the repeated evolution of masseter architectures. *Proc Biol Sci*. 2019;286(1902):20190672.
34. Davis CA, Hitz BC, Sloan CA, Chan ET, Davidson JM, Gabdank I, Hilton JA, Jain K, Baymuradov UK, Narayanan AK, Narayanan AK, Davis CA, Hitz BC, Sloan CA, Chan ET, Davidson JM, Gabdank I, Hilton JA, Jain K, Baymuradov UK, Narayanan AK, Onate KC, Graham K, Miyasato SR, Dreszer TR, Strattan J, Jolanki O, Tanaka FY, Cherry J. The Encyclopedia of DNA elements (ENCODE): data portal update. *Nucleic Acids Res*. 2018;46(D1):D794–801. <https://doi.org/10.1093/nar/gkx1081>.
35. Mirdita M, Schütze K, Moriawaki Y, Heo L, Ovchinnikov S, Steinegger M. ColabFold: making protein folding accessible to all. *Nat Methods*. 2022;19(6):679–82. <https://doi.org/10.1038/s41592-022-01488-1>.
36. Kumar S, Stecher G, Li M, Knyaz C, Tamura K. MEGA X: Molecular Evolutionary Genetics Analysis across Computing Platforms. *Mol Biol Evol*. 2018;35(6):1547–9. <https://doi.org/10.1093/molbev/msy096>.
37. Edgar RC. MUSCLE: multiple sequence alignment with high accuracy and high throughput. *Nucleic Acids Res*. 2004;32(5):1792–7. <https://doi.org/10.1093/nar/gkh340>.
38. Korber B. HIV signature and sequence variation analysis. Computational analysis of HIV Molecular sequences. Dordrecht: Kluwer Academic Publishers; 2000.

## Publisher's Note

Springer Nature remains neutral with regard to jurisdictional claims in published maps and institutional affiliations.

Ready to submit your research? Choose BMC and benefit from:

- fast, convenient online submission
- thorough peer review by experienced researchers in your field
- rapid publication on acceptance
- support for research data, including large and complex data types
- gold Open Access which fosters wider collaboration and increased citations
- maximum visibility for your research: over 100M website views per year

At BMC, research is always in progress.

Learn more [biomedcentral.com/submissions](https://biomedcentral.com/submissions)

